SMAR 2015 – Third Conference on Smart Monitoring,
Assessment and Rehabilitation of Civil Structures

Numerical modeling of ferrocement-strengthened RC beams

Usama Ebead[1]

[1] Qatar University, Doha, Qatar

ABSTRACT: An experimental study was recently published by the author that presented a research that constituted a special importance for developing countries where an affordable trowel-based ferrocement-strengthening system was adopted for reinforced concrete beams. The beams were cast, pre-loaded to different load fractions (45% and 60%) of its ultimate capacity and then the load was partially released (by 15% of the ultimate load) and maintained while the beams were then ferrocement-strengthened and reloaded until failure. The released load simulates the removed live load while strengthening an actual beam.

Finite element simulations of this application will be presented here to complement the aforementioned research work. The full understanding of the flexural behavior of ferrocement-strengthened beams necessitates creating numerical models, of which results are substantiated by experimental findings. The models are developed to assess the flexural behavior of beams strengthened using two different schemes; namely, flat shaped and U-shaped ferrocement-strengthened beams. The behaviour of the ferrocement in tension will be obtained based on available experimental model developed by the author as part of the material characterization of the utilized materials. Results will be presented in terms of the ultimate load capacities, and load-deflection relationships. Numerical results will be validated against the published experimental results.

1 INTRODUCTION

The utilization of cementitious composite materials has been presented in several contributions (Maalej and Leong 2005, Shannag and Al-Ateek 2006, Ombres 2011, Hashemi and Al-Mahaidi 2012, Hussein, Kunieda et al. 2012, Maalej, Quek et al. 2012, Ombres 2012). Steel-reinforced strain hardening cementitious composites were used for concrete beam strengthening and contributed to improving the ductility of the beams (Hussein, Kunieda et al. 2012). Moreover, an experimental work was recently focused on renewing interest in utilizing ferrocement as a viable, economic, and suitable strengthening technique for concrete structural elements in developing countries where cost is an important factor (Ebead 2015).

The determination of the structural behavior of strengthened structures requires advanced numerical methods of which results are substantiated by credible experimental findings. Researchers have employed finite element packages to investigate the structural behavior of both passive and strengthened concrete beams where the bond between the strengthening materials and concrete is accounted for and modeled (Kotynia, Baky et al. 2008, Elsayed, Ebead et al. 2009, Ebead and Saeed 2014). In the literature, a successful approach has been used to simulate debonding modes of failure and to predict the associated debonding loads using finite element analysis (Elsayed, Ebead et al. 2009, Ebead and Saeed 2014). In such an approach,

discrete interface elements having a predefined interfacial shear stress-slip (bond-slip) relation are used to link the FRP and concrete elements. Stress concentrations along the interface between the strengthened length between the strengthened materials and concrete interface in the vicinity of cracks can be predicted by using such discrete interface elements. Continuous interface elements, however, use a continuous interpolation function for the interface so that the stress fields are assumed constant, contrary to the fact that there is a stress concentration at the crack tips as seen in (Ebead and Neale 2007). Ebead and Neale used the discrete interface elements to define the interfacial behavior of the basic direct shear application of FRP-concrete joints (Ebead and Neale 2007). These elements have also been successfully adopted in several other two- and three-dimensional finite element applications of FRP EB RC beams and slabs (Neale, Ebead et al. 2006, Baky, Ebead et al. 2007, Elsayed, Ebead et al. 2007, Kotynia, Baky et al. 2008, Ebead and Saeed 2010).

Ongoing research efforts are being carried out by the author where renewed interests in the use of cementitious material composites are used in strengthening of reinforced concrete elements. These efforts include also developing rigorous finite element models for the analysis of the strengthened specimens. In this presented work, finite element models are created to investigate the flexural behaviour of the ferrocement strengthened beams. In more ongoing sophisticated modelling efforts by the author, the interfacial behaviour is accounted for. Here, in this research paper, full bond between the concrete beam and the ferrocement is enforced.

Therefore, an experimental investigation on the strengthening of RC beams using ferrocement has been conducted, and the results have been published by Ebead (Ebead 2015). The research presented herein features modelling the flexural behaviour of concrete beams. The beams have been preloaded prior to strengthening and this effect will be accounted for in the presented work. One of the features of this work is incorporating the microplane theory for concrete modeling.

2 SUMMARY OF THE EXPERIMENTAL PROGRAM ON FERROCEMENT STRENGTHENED BEAMS

Twelve (12) reinforced concrete strengthened specimens and a control specimen were tested. The beam dimensions were 2,400 mm in length × 120 mm in width × 200 mm in height. A cover of 20 mm was maintained between the center of the main steel reinforcement and the concrete surface. The beams were loaded as a double cantilever with a distance between the supports of 500 mm and total loaded span of 2,200 mm. The thickness of the ferrocement layer was 25 mm. Three different parameters have been altered to examine their effects on the flexural behaviour of the strengthened specimens. These parameters were the volume fraction of the ferrocement, the strengthening scheme and the pre-loading level. **Figure 1** shows a schematic drawing of a beam. This figure also shows the dimension, reinforcing details and cross sectional details of the control and the strengthened beams.

In the original experimental work, for the ferrocement mortar, the cement-to-sand weight ratio is 0.5, water-to-cement ratio is 0.40, and the dosage of the superplasticizer is 0.45% of the cement content by weight. The expanded metal mesh used has the following properties: the weight/m^2 is 3.5 kg, and strand width × thickness are 2.4 × 1.25 mm.

As per Column 4 in **Table 1**, the volume fraction for Specimens BU1 through BU4, BF5 through BU8 and BF9 through BU12 was 5.45%, 2.80%, and 0.98%, respectively. Two strengthening schemes were evaluated in this research work where flat and U-shaped ferrocement layers were used. As listed in **Table 1**, Specimens BF2, BF3, BF5, BF6, BF9, and BF10 were strengthened using flat-shaped ferrocement layers, while beams BU1, BU4, BU7,

BU8, BU11, and BU12 were strengthened using U-shaped ferrocement layers. Two pre-loading levels were assessed to simulate two cases; namely repair and strengthening by applying two different levels of damage. These two pre-loading levels were 45% and 60% of the ultimate load of the control specimen, BC, for the strengthening and repair situations, respectively.

Table 1: Concrete properties and numerical versus experimental results

1	2	3	4	5	6	7	8	9	10
ID	f_c', MPa	f_t', MPa	VF, %	P_y,exp. kN	P_y,num. kN	P_y,num. /P_y,exp.	P_u,exp. kN	P_u,num .kN	P_u, num. / P_u, exp.
BC	35	2.7	NA	9.1	10.5	1.15	12.2	12.5	1.02
BU1	34	2.9	5.45	15.1	18.9	1.25	26.6	29.4	1.11
BF2	34	2.8	5.45	11.8	13.9	1.18	19.1	20.3	1.07
BF3	36	2.7	5.45	11.2	13.8	1.23	18.3	20.2	1.11
BU4	35	2.9	5.45	14.5	19	1.31	25.9	30.9	1.19
BF5	34	2.7	2.80	11.6	12.3	1.06	15.1	17.8	1.18
BF6	33	2.8	2.80	11.1	12.3	1.11	14.9	17	1.14
BU7	35	2.6	2.80	13.5	16.1	1.19	19.5	22.2	1.14
BU8	36	2.9	2.80	13.3	16.1	1.21	21.1	22.2	1.06
BF9	36	3.1	0.98	8.9	9.8	1.1	11.5	13.9	1.21
BF10	35	2.7	0.98	8.6	9.8	1.14	11.4	13.1	1.15
BU11	34	3.1	0.98	11.2	13.7	1.22	14.2	16.1	1.14
BU12	36	3.1	0.98	11.1	13.7	1.23	14.9	16.9	1.14

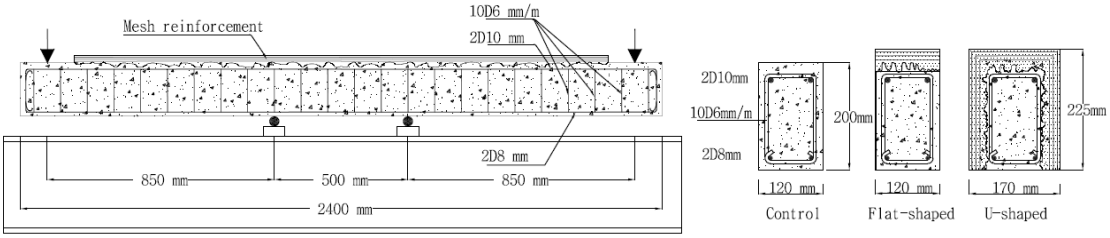

Figure 1. Beam characteristics and dimensions.

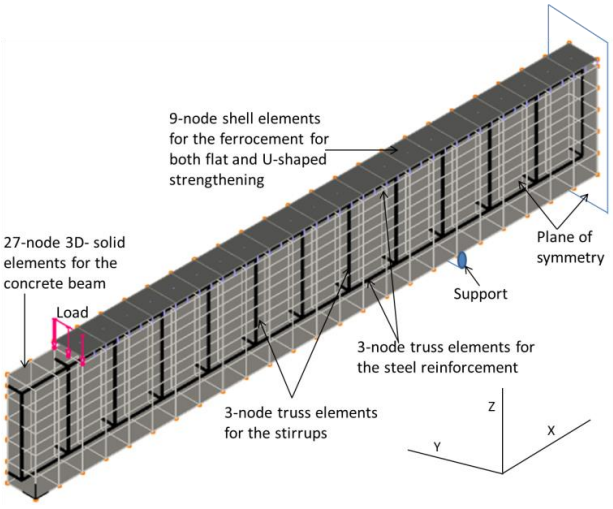

Figure 2. Finite element model for a flat-shaped strengthened specimen.

3 FINITE ELEMENT MODELLING

The numerical analysis is carried out using the finite element software package ADINA (Bathe 2005). The concrete compressive and tensile strengths for each specimen as obtained from the original experimental work (Ebead 2015) are listed in **Table 1** are used in the material model definition. Description of the material modelling, finite elements used and the simulated boundary conditions are presented hereafter.

3.1 Material modelling of the concrete

The M4 version of the microplane model is used to define the concrete constitutive behaviour (Caner and Bažant 2000). The basic assumption of the microplane approach is that the microstrains at a plane are constrained to the macrostrains at an integration point represented by a volume containing a number of planes. This is referred to as "the kinematic constraint" that gives the microstrains as the projection of the macrostrain tensor on microplanes,

$$\varepsilon_N = N_{ij}\varepsilon_{ij},\ \varepsilon_M = M_{ij}\varepsilon_{ij},\ \varepsilon_L = L_{ij}\varepsilon_{ij}, \tag{1}$$

where ε_{ij} is the component ij of the strain tensor, ε_N is the normal strain and ε_L and ε_M are the tangential strains along orthogonal axes on the microplanes (the components of the shear microstrains). Therefore, N_{ij}, M_{ij}, and L_{ij} are the transformation matrices used to project the ε_{ij} tensor on a microplane to obtain the normal and shear microstrains. The normal microstrain vector is composed of volumetric (ε_V) and deviatoric (ε_D) strain vectors; i.e.,

$$\varepsilon_N = \varepsilon_V + \varepsilon_D \tag{2}$$

The magnitude of the shear strain ε_T is given by:

$$\varepsilon_T = \sqrt{\varepsilon_L{}^2 + \varepsilon_M{}^2} \tag{3}$$

The micro stresses on each microplane are determined from stress–strain relationships developed for a generic microplane. The micro stresses are then combined using the principle of virtual work to obtain the macro stress tensor at a point. The characteristics of concrete used in the material definition were based on the experimental work. Numerous general constants for defining the concrete constitutive model were given as per Caner and Bažant (2000).

3.2 Material modelling of the steel reinforcing bars

The longitudinal and transverse steel reinforcement bars are modelled as bilinear elastic-plastic materials, with the tangent modulus in the strain-hardening zone is taken to be 1/100 of the elastic modulus. Properties of the steel reinforcement are based on the original experimental work (Ebead 2015). The yield stresses for the steel reinforcement bars as given in the original reference are 420 MPa for the main top reinforcement and 260MPa for both the secondary reinforcement and the stirrups.

3.3 Material modelling of the ferrocement layer

3.3.1 Stress- strain relationship for ferrocement in tension

Based on the experimental results of tensile testing of ferrocement, it was possible to derive a general template for the stress-strain relationship of which parameters depend on the volume fraction. A best-fit based stress-strain relationship is as follows:

For 0 <ε < 120e-6, slope = 12500 $VF^{0.53}$ (MPa) (4)

For 120e-6 <ε < 2200e-6, slope = 1400 $VF^{0.65}$ (MPa) (5)

For 2200e-6 <ε, failure occurs in the ferrocement layer (6)

3.3.2 Stress- strain relationship for ferrocement in compression

The effect of longitudinally oriented mesh reinforcement on the load-deformation relationship and therefore the stress-strain relationship in compression is minimal. When the reinforcement is in one direction only, it has a minimal effect on the load-deformation relationship, and the associated elastic modulus remains virtually the same as that for the mortar matrix (Pama, Sutharatnachaiyarorn et al. 1974). Therefore, a concrete constitutive model in compression will be used to define the uniaxial compression stress-strain relationship. The model of Kent and Partk (1971) is used here to define ferrocement behaviour in compression. The compressive stress strain is divided into three portions, ascending, descending and constant. For the ascending portion, the stress strain relationship is defined as:

For $0 < \varepsilon < 0.002$ $$f = f_c' \left[\left(\frac{2\varepsilon}{0.002}\right) - \left(\frac{\varepsilon}{0.002}\right)^2\right] \quad (7)$$

For the descending part:

For $0.002 \geq \varepsilon$ $$f = f_c'[1 - Z_m(\varepsilon_c - 0.002)] > f_{res}. \quad (8)$$

Where,

$$Z_m = \frac{0.5}{\frac{3 + 0.29 f_c'}{145 f_c' - 1000}} \quad (9)$$

For the residual stresses represented by the constant portion:

$$f = f_{res} = 0.2 f_c' \quad (10)$$

3.4 Geometrical Modelling, Loading and Boundary Conditions

Essential three-dimensional models are created strengthening application, particularly for the inverted U-shape strengthening application. Therefore, for the entire specimens, three dimensional models were created. Only one quarter of a beam specimen is modelled to take advantage of the loading and geometrical symmetry with respect to a longitudinal place intersection mid-width of the beam. As shown in **Figure 2**, three-dimensional 27-node brick elements with three degrees of freedom per node are employed to define the concrete beams.

The minimum node-to-node distance was 25 mm which is considered appropriate for such an application. The steel reinforcement bars in the longitudinal and transverse directions are represented using 3-node truss elements. Each element has two translational degrees of freedom at each node. The nodes of these truss elements have full constraint compatibility with the in-common nodes of the 3-D concrete elements, i.e., full bond between the concrete and the steel reinforcement is enforced. Nine-node shell elements with three degrees of freedom at each node are used for the ferrocement layer. Full strain compatibility is enforced between the ferrocement and the concrete nodes in both the longitudinal and normal direction.
The sustained preloading level was accounted for in this model. For the control specimen, loads were defined to be applied linerly until the solution is complete. Based on this analysis, the load levels at which the beam is loaded upto 45% and 60% of ultimate load of the control specimen is marked. For the strengthened specimens, the ferrocement shell elements are only activiated at the specified preloading level, either 45% or 60% of the ultimate load of the control specimen.

4 NUMERICAL RESULTS AND DISCUSSIONS

4.1 Yield Loads, Ultimate load capacities, deflections, and modes of failure

The load at which the tension reinforcement started to yield is considered the yield load. It is found that the model overestimates the yield load values as compared to the reported experimental results by 19% with a standard deviation of 7% as listed in **Table 1** where the numerical and experimental yield loads, $P_{y,num.}$,and $P_{y,exp.}$, respectively, are listed. The over estimation of the yield load was partially a result of the effect of the sustained loading for the physical beams during the period from applying the strengthening material to testing the beams. Such an effect would indeed weaken the beams and accelerating steel yielding (Ebead 2015). Such an effect was not captured in the numerical modelling.The experimental results of 13 specimens have been used to validate the finite element models that have accurately predicted the ultimate load capacities for the simulated beams as shown in the comparisons in **Table 1.** The predictions ranged between 102 and 121% with an average of 113% and a standard deviation of 5.0%, which indicates an overestimation of the numerical and the experimental load capacities, $P_{u,num.}$ As compared to the reported experimental results $P_{u,exp.}$. It is beleived that the overestimation of the ultimate loads is due to ignorig the interfacial behaviour between the ferrocement and the concrete beam.
The graphs in **Figure 3a** through **Figure 3f** depict the entire load–deflection scatter for all strengthened specimens (Ebead 2015) versus the finite element predicted plateaus. The models predicted the load–deflection scatters with an average overestimation of about 12% for the specimens strengthened using ferrocement layer with volume fraction 5.45% for the U-shaped and flat strengthening for specimens as in **Figure 3a** and **b**, respectively. For the specimens with ferrocement with volume fraction of 2.8%, the models also predicted the load deflection scatter up to failure with also an overestimation of an average 13% as per **Figures 3c** and **3d**. The models did not capture the weakening effect of preloading for the specimens strengthened with ferrocement of volume fraction of 0.98% shown in **Figures 3e** and **3f**. It is indicated here that defining the interfacial behaviour between the strengthening matetrial will lead to better prediction as reported in other research work efforts (Ebead and Saeed 2014).
The numerical results showed that all of the specimens reached steel reinforcement yield earlier than reaching the ultimate load capacity. This indicates that the mode of failure for all of the specimens is flexure type of failure. This is actually consistent with the reported experimental results.

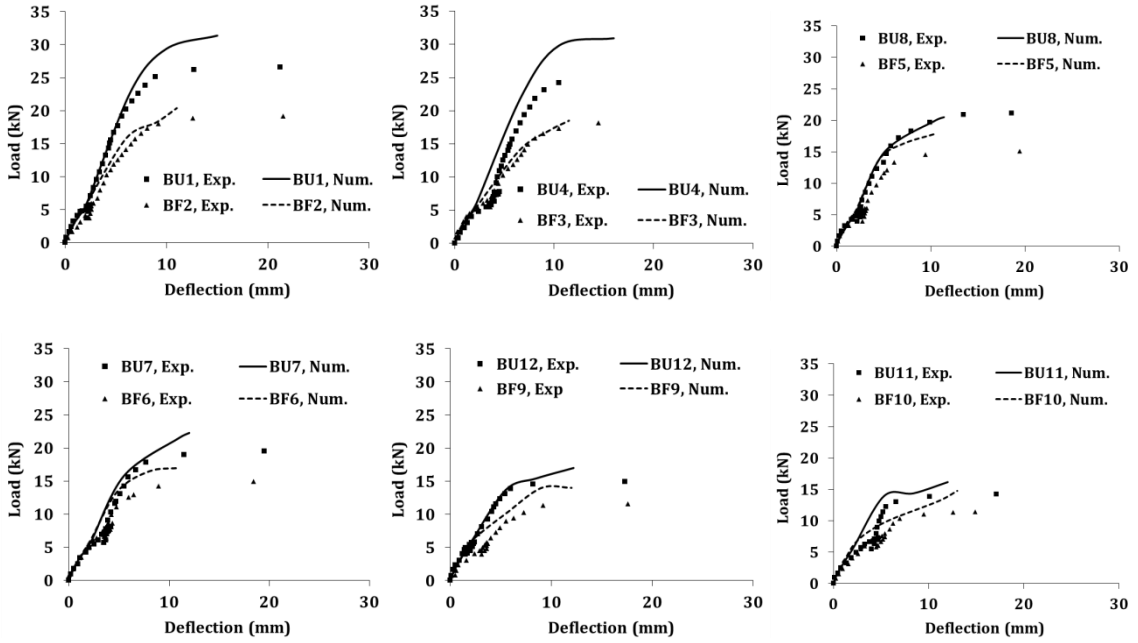

Figure 3. Numerical versus experimental load-deflection relationships for the entire specimens.

5 CONCLUSION

In this research the flexural behaviour of ferrocement strengthened beams has been numerically studied through finite element modelling of thirteen beam specimens. Finite element models of reinforced concrete beams strengthened using ferrocement composites were created. Available experimental results were used to verify the models. The strengthened beams were classified according to strengthening scheme as flat- and U-shaped ferrocement-strengthened specimens. The concrete microplane model was used as a user-defined subroutine in the finite element package. The predictions of the yield loads and ultimate load capacities were fairly accurate when compared with the available experimental results for 13 specimens; those include a reference and 12 strengthened specimens. The average numerical to experimental yield and ultimate loads are 1.056 and 1.16, with standard deviations of 19 and 4%, respectively. This indicates the prediction quality of the model in estimating these loads with reasonable accuracy. In addition, the model fairly accurately predicted the entire load-deflection plateaus for the entire aforementioned 13 specimens. Considering the interfacial behaviour between the concrete and ferrocement is beleived to improve ultimate load predictibility of the numerical models. It was also concluded from the results that the dominating mode of failure is flexure, which is consistent with the experimental results.

6 ACKNOWLEDGEMENT

This paper was made possible by NPRP grant # NPRP 7-1720-2-641 from the Qatar National Research Fund (a member of Qatar Foundation). The statements made herein are solely the responsibility of the author.

7 REFERENCES

Baky, H. A., U. A. Ebead and K. W. Neale (2007). "Flexural and interfacial behavior of FRP-strengthened reinforced concrete beams." *Journal of Composites for Construction* 11(6): 629-639.

Bathe, K. J. (2005). ADINA. Watertown, MA, USA, ADINA R & D, Inc.

Caner, F. and Z. Bažant (2000). "Microplane model M4 for concrete. II: Algorithm and calibration." Journal of Engineering Mechanics 126(9): 954-961.

Ebead, U. (2015). "Inexpensive Strengthening Technique for Partially Loaded Reinforced Concrete Beams: Experimental Study." *Journal of Materials in Civil Engineering* 10.1061/(ASCE)MT.1943-5533.0001249 , 04015002.

Ebead, U. and K. Neale (2007). "Mechanics of fibre-reinforced polymer-concrete interfaces." *Canadian Journal of Civil Engineering* 34(3): 367-377.

Ebead, U. and H. Saeed (2010). "Modeling of reinforced concrete slabs strengthened with fiber-reinforced polymer or steel plates." *ACI Structural Journal* 107(02): 218-227.

Ebead, U. and H. Saeed (2014). "Flexural and Interfacial Behavior of Externally Bonded/Mechanically Fastened Fiber-Reinforced Polymer Strengthened Reinforced Concrete Beams." *ACI Structural Journal* 111(4): 741-752.

Ebead, U. and H. Saeed (2014). "Numerical Modeling of Shear Strengthened Reinforced Concrete Beams Using Different Systems." Journal of Composites for Construction 18(1): 04013031.

Elsayed, W., U. A. Ebead and K. W. Neale (2007). "Interfacial behavior and debonding failures in FRP-strengthened concrete slabs." *Journal of Composites for Construction* 11(6): 619-628.

Elsayed, W. E., U. A. Ebead and K. W. Neale (2009). "Mechanically Fastened FRP-Strengthened Two-Way Concrete Slabs with and without Cutouts." *Journal of Composites for Construction* 13(3): 198-207.

Hashemi, S. and R. Al-Mahaidi (2012). "Experimental and finite element analysis of flexural behavior of FRP-strengthened RC beams using cement-based adhesives." *Construction and Building Materials* 26(1): 268-273.

Hussein, M., M. Kunieda and H. Nakamura (2012). "Strength and ductility of RC beams strengthened with steel-reinforced strain hardening cementitious composites." *Cement and Concrete Composites* 34(9): 1061-1066.

Kent, D. C. and R. Park (1971). "Flexural members with confined concrete." *Journal of the Structural Division* 97(7): 1969-1990.

Kotynia, R., H. A. Baky, K. W. Neale and U. A. Ebead (2008). "Flexural strengthening of RC beams with externally bonded CFRP systems: Test results and 3D nonlinear FE analysis." *Journal of Composites for Construction* 12(2): 190-201.

Maalej, M. and K. S. Leong (2005). "Engineered cementitious composites for effective FRP-strengthening of RC beams." *Composites Science and Technology* 65(7–8): 1120-1128.

Maalej, M., S. T. Quek, S. F. U. Ahmed, J. Zhang, V. W. J. Lin and K. S. Leong (2012). "Review of potential structural applications of hybrid fiber Engineered Cementitious Composites." *Construction and Building Materials* 36(0): 216-227.

Neale, K., U. Ebead, H. A. Baky, W. Elsayed and A. Godat (2006). "Analysis of the load-deformation behaviour and debonding for FRP-strengthened concrete structures." *Advances in Structural Engineering* 9(6): 751-763.

Ombres, L. (2011). "Flexural analysis of reinforced concrete beams strengthened with a cement based high strength composite material." *Composite Structures* 94(1): 143-155.

Ombres, L. (2012). "Debonding analysis of reinforced concrete beams strengthened with fibre reinforced cementitious mortar." *Engineering Fracture Mechanics* 81(0): 94-109.

Pama, R., C. Sutharatnachaiyarorn and S. Lee (1974). Rigidities and strength of ferrocement. *First Australian Conference on Engineering Materials*, University of New South Wales, Sydney, Australia.

Shannag, M. J. and S. A. Al-Ateek (2006). "Flexural behavior of strengthened concrete beams with corroding reinforcement." *Construction and Building Materials* 20(9): 834-840.